Supplementary text, figures and tables for Clog et al "A reconnaissance study..."

1 Details of notation

1.1 Bulk isotope ratios

Bulk isotope ratios (i.e., inventories of rare isotopes, independent of the isotopologue in which they occur) are reported using the delta notation, defined as follows:

$\delta = 1000 \text{ x } (R/R_{ref} - 1)$

where R is the ratio of [D]/[H] for hydrogen and $[^{13}C]/[^{12}C]$ for carbon. R_{ref} refers to the standard to which the isotopic composition of the sample is compared. In this study, the reference for hydrogen is V-SMOW and the reference for carbon is V-PDB.

Typically, reported bulk isotopic compositions either ignore multiply-substituted isotopologues or assume that the distribution of isotopes is random among isotopologues (for example in the determination of δD from H_2, D_2 is ignored and the ratio of $[DH]/[H_2]$ is used. For CO_2, the rare isotopologues on masses 47, 48, and 49 or the doubly substituted isotopologues on mass 46, $^{13}C^{17}O^{16}O$ and $^{12}C^{17}O_2$ are not taken into account to calculate the isotopic composition in carbon and oxygen). This is generally a reasonable

assumption for natural samples due to the low abundance of heavy isotopes for these elements. The multiply-substituted isotopologues are not numerous enough in these cases to matter for the determination of the bulk isotopic compositions, for a worked example see [Stolper et al., 014a].

2 Mass spectrometry details

2.1 Justification of the choice of ions to measure

Although the mass with the highest signal in the mass spectrum corresponds to m/z = 28 (chiefly $C_2H_4^+$, i.e., an ethane molecule which has lost 2 H atoms in the ion source of the mass spectrometer), it is not convenient to measure C_2H_4 and its substituted isotopologues. It is possible to formally resolve $^{13}C_2H_4$ from $^{12}C_2H_6$ at m/z = 30, and indeed its amplitude is higher than that of $^{13}C_2H_6$ at m/z = 32, but doing so requires challenging background corrections associated with the peak tailing of $^{12}C_2H_6$, which is several orders of magnitude more intense than adjacent $^{13}C_2H_4$. We therefore focus on the isotopologues of $C_2H_6^+$ at m/z equal to 30 (no heavy isotope), 31 (containing either ^{13}C or D, and possibly H-adducts of the mass 30 isotopologues), and 32 (two ^{13}C, two D, or one each, and possibly H-adducts of the mass 31 isotopologues).

2.2 Ionization spectrum

Figure S1 presents a scan of the full mass spectrum of ethane measured on the Ultra with source conditions tuned to optimise signal on mass 30 (C_2H_6 and isobars that are visually indistinguishable at the plotted scale). Compared to a simple molecule like CO_2, ethane has a complex mass spectrum due

to the presence of diverse fragment ions, including H loss from the parent C_2H_6, and methyl ion fragments that gain or lose H through fragmentation or adduction. +2 charge ions are also observed.

2.2.1 Mass 30

The most intense ion present near mass 30 amu is $C_2H_6^+$, less intense — typically less than 2 percent, total — are the singly-substituted isotopologues of the fragment ion, $C_2H_5^+$ ($^{13}C^{12}CH_5^+$ and $^{12}C_2H_4D^+$, resulting from the loss of one of the hydrogen atoms from the full molecule during ionisation). Other isobaric species are not detected when scanning across this family of peaks and registering signals with a Faraday cup read through a 10^{11} Ω amplifier (see Figure S2). Mass scans of the low-mass side of this set of peaks with an electron multiplier reveals weak signals from the doubly-substituted fragments ions having the stoichiometry, C_2H_4+, including $^{13}C_2H_4^+$, $^{13}C^{12}CDH_3^+$ and $^{12}C_2D_2H_2^+$. The sum of the intensities of these isotopologues is 4 orders of magnitude lower than the intensity of the main beam, $^{12}C_2H_6+$. Rather than trying to mass resolve the singly and doubly substituted fragment ions by measuring the intensity of the mass 30 beam on the high-mass shoulder (see Figure S2), it is more practical to measure the sum of $^{12}C_2H_6^+$, $^{13}CCH_5^+$, $^{12}C_2H_4D^+$, $^{13}C_2H_4^+$, $^{13}C^{12}CDH_3^+$ and $^{12}C_2D_2H_2^+$. The last three can be ignored as their abundance is very low, and we correct for the abundance of $^{13}CCH_5^+$ and $^{12}C_2H_4D^+$ during data processing, as detailed in the appendix. Finally, traces of ions such as $^{12}C^{18}O^+$ or $^{14}N^{16}O^+$ must be present and the resolution of the instrument would be sufficient to resolve them, but they are not detected even with SEM scans of the mass range of interest, and we do not attempt to

correct for these species.

2.2.2 Mass 31

The main ions present on mass 31 are $^{13}C^{12}CH_6^+$ and $^{12}C_2DH_5^+$, with a minor contribution from the fragments of doubly-substituted isotopologues ($^{13}C_2H_5^+$, $^{13}C^{12}CDH_4^+$ and $^{12}C_2D_2H_3^+$). No other isobaric species are observed when this part of the mass spectrum is registered through a Faraday cup with a 10^{12} Ω amplifier (Figure S3), and the fragments of doubly-substituted isotopologues bearing one or two D, although present, are not visible. Importantly, there is no evidence for the presence of an adduct species, i.e. $^{12}C_2H_7^+$. As shown in Table S1 as well as in the Adducts subsection in this document, there is no relationship between the intensity of the signal at mass 30 and the measured $\delta^{13}C$ and δD, which shows that even if adduct species are present they are negligible. In high-resolution mode (5 μm entrance slit, mass resolving power ~22,500), it is possible to completely resolve $^{13}C^{12}CH_6$ from $^{12}C_2DH_5$ by measuring on the leading shoulder (as shown on Figure S3). The first measurement ('measurement 1' in Figure S3) gives:

$$i_{31\text{-A}} = i^{^{13}C^{12}CH_6} + i^{^{12}C_2DH_5}$$

while the second ('measurement 2' in Figure S3) gives

$$i_{31\text{-B}} = i^{^{13}C^{12}CH_6}$$

These two measurements allow us to constrain the bulk isotopic composition of ethane (both δD and $\delta^{13}C$), after correction for the presence of fragment species (see Comparison with classical techniques for the external validation and the Appendix for the details of the calculations).

2.2.3 Mass 32

The mass 32 mass spectrum is measured on an electron multiplier. We can identify signals from O_2^+, CH_3OH^+, $^{13}C_2H_6^+$ and $^{13}C^{12}CDH_5^+$ (see Figure S4). $^{12}C_2D_2H_4^+$ is also recognised but not visible at the scale at which Figure S4 is plotted. Fragments of heavier ethane isotopologues, such as $^{13}C_2DH_4^+$ must be present but are very low in abundance ($<0.01\%$) and are thus not recognisable given the integration time at each mass for the illustrated scan, and in any case are negligible for the purposes of our measurements. Likewise, we do not observe the presence of $^{14}N^{18}O^+$ or other possible isobaric contaminants.

In high-resolution mode, O_2^+ ions are completely resolved from the ions derived from the isotopologues of ethane. It is also possible to measure the abundance of $^{13}C_2H_6^+$ independently from the other doubly-substituted isotopologues of ethane. However, the CH_3OH^+ beam overlaps the low-mass side of the $^{13}C_2H_6^+$ shoulder (see Figure S4) due to the wide aperture of the detectors used for these measurements. Thus, any measurement made on the low mass side of the mass 32 ethane peak must correct for methanol interference.

Methanol is not a contaminant from our samples, and is present at comparable ion intensities when measuring aliquots of pure commercial ethane and aliquots prepared by purification and concentration of ethane from natural samples. Samples are typically introduced in the bellows of the instrument using glass break-seals, and keeping the end of these tubes immersed in a dry ice-ethanol slush, which would prevent methanol from leaving the break-seal, does not impact the amount observed on mass 32. We also observed that when the H_2O background signal was higher, the relative amount

of methanol ions was higher. Methanol is most likely produced by reaction of ethane or of the methyl fragment with trace amounts of water that are always present in the source of the mass spectrometer through reactions such as:

$C_2H_6^+ + H_2O = CH_3OH^+ + CH_4$

or

$CH_3^+ + H_2O = CH_3OH^+ + H$

Typically, CH_3OH+ represents 2 to 5% of the measured signal at mass 32. It is corrected by measuring CH_3OH^+ alone (at a typical intensity of $\approx$ 3000 counts per second) and subtracting its measuring intensity from the measured intensity of ($^{13}C_2H_6^+ + CH_3OH^+$) (at a typical intensity of 60,000 counts per second; see next section for details of the analytical sequence). To obtain precisions for $\Delta^{13}C_2H_6$ of $\pm$ 0.12‰, counting time of $\approx$2400 s are required for both the reference gas and the sample. This step of the measurement most strongly controls the overall speed of each analysis.

2.3 Evidence for negligible adduct species

It is imaginable such adduct species could form in the source of the mass spectrometer, much as they do during conventional mass spectrometric analyses of H_2, through the reaction:

$H_2 + H_2^+ = H + H_3^+$

[Friedman, 1953]. A similar phenomenon occurs in mass spectrometric analysis of methane [Stolper et al., 014a]. If such adducts were present in the part of the ethane mass spectrum on which we focus it would be necessary to mass resolve them or correct for their presence. Although we do not recognise the presence of an adduct species on the mass scans performed

on mass 31, this is a sufficiently important question that we conducted an experiment to look for indirect evidence that it is present, not mass resolved, and significant enough in intensity to lead to analytical artefacts.

H adducts on H_2 and CH_4 have been recognised and empirically corrected for by observing a dependence of the raw measured ratio of isotopologues (e.g., mass 3/mass 2 for H_2) depends on source pressure, which is correlated with the intensity of the major ion beam (i.e., mass 2 for H_2). Likewise, we searched for the indirect evidence of adducts by determining the dependence of the mass 31/mass 30 ratio on the signal intensity of mass 30. No significant correlation between these two variables was observed. We searched further for indirect evidence of artefacts associated with adducts by determining if there is a dependence of the sample/standard difference in 31/30 ratio on source pressure (as measured by signal 30 intensity). The rationale behind this test is that, if adducts form in some fashion that depends on source pressure (as they do for H_2 and CH_4), then they will create a form of 'scale compression', where the difference in apparent isotope ratio between two gases that differ in isotopic composition will diminish as the abundance of adducts increases. And, even if no dependence on source pressure is detected, if we independently know the isotopic composition (i.e., δD and δ^{13}C) of both gases being compared, the presence of adducts should be revealed by measured differences that are smaller than expected. Table S1 presents results from the comparison of two gases with known isotopic compositions (see the 'Experimental Reproductibility' section for details). We see no evidence for a compression in the scale of isotopic variation at any source pressure investigated. We conclude that adducts are absent or so low in abundance that they have no measurable effect on the 31/30 ratio. It follows that the intensity measured on top of the composite peak at mass 31

equals the sum of the intensities of the ion beams for the singly-substituted isotopologues of ethane, $^{13}C^{12}CH_6^+$ and $^{12}C_2DH_5^+$, plus a minor contribution from fragments of doubly-substituted molecules.

2.4 Fragmentation ratio

On both mass 30 and 31, there are non-negligible amounts of fragments of the whole ethane molecule, bearing one or two heavy isotopes. Although it is possible to measure the intensity of $^{12}C_2H_6^+$ without the fragments, we found that it is more practical to correct for their abundances, and that this approach leads to no obvious analytical artefacts. Moreover, on mass 31, it is not possible to measure the intensity of $^{13}C^{12}CH_6^+$ without interference from either fragments of the doubly-substituted isotopologues or $^{12}C_2DH_5^+$ (see Figure S3). As with many other interferences noted in this study, this arises not from a lack of mass resolution, but because of the presence of interfering masses to both high and low mass side of a beam of interest, and the use of wide detector apertures to promote the high precision that is possible with flat-topped peaks. One solution to this issue would be to make all of the measurements we describe with narrow exit slits. This may be advantageous (though we find no evidence in this study that it would be particularly effective at improving overall data quality), though any such effort would likely have to contend with the challenges of measuring precise isotope ratios on narrow, partly rounded peaks.

To correct for the fragmentation, we measure the ion intensity of ethane signals on mass 29 and 30. Mass 29 includes $^{12}C_2H_5^+$, which represents more than 95% of the signal, as well as $^{13}C^{12}CH_4^+$ and $^{12}C_2DH_3^+$. Mass 30 includes $^{12}C_2H_6^+$ (98% of the signal) and both $^{13}C^{12}CH_5^+$ and $^{12}C_2DH_4^+$. It

is possible to measure only the ratio of $^{12}C_2H_6^+$ to $^{12}C_2H_5^+$, excluding the fragments, but this necessitates either peak-hopping or changing the configuration of the collector array. Moreover, we found that the final calculated values for the isotopic compositions are not sensitive to small variations in the value of the fragmentation correction. The mass 29 to mass 30 ratio is generally of ≈0.81, with a range of ± 0.025 observed over 18 months of measurements. The determination of the fragmentation ratio, noted F, is conducted at the same source tuning conditions and same source pressure at which the measurements are performed. We assume for the remainder of this method that F is constant through time, constant across source conditions typical of our measurements, and identical for all isotopologues of interest. Note that to create an error on δD or δ^{13}C larger than the standard error of one analysis, F must be wrong by more than 25%, relative. Thus, the approximations we adopt out of convenience appear to be justified and unlikely to lead to analytical artefacts.

3 Details of the measurement procedure

3.1 Measurement 1 details

We first configure the detector array of the Ultra to measure simultaneously the ratios of

$(^{13}C_2H_6^+ + {}^{12}CH_3OH^+)$ to $(^{12}C_2H_6^+ + {}^{13}C^{12}CH_5^+ + {}^{12}C_2DH_4^+)$

and

$(^{13}C^{12}CH_6^+ + {}^{12}C_2DH_5^+ + {}^{13}C_2H_5^+ + {}^{13}C^{12}CDH_4^+)$ to $(^{12}C_2H_6^+ + {}^{13}C^{12}CH_5^+ + {}^{12}C_2DH_4^+)$.

The methanol ion contributions are removed by background correction, and the contributions from fragments are corrected during the data process-

ing using the fragmentation rate F (see the fragmentation subsection in this document). The contributions from $^{12}C_2D_2H_3^+$ are neglected due to its very low abundance. The differences between the sample and the reference are described using δ notation, with

$$\delta^{13}C_2H_6 = 1000 \; . \; (^{^{13}C_2H_6}R_{sample}/^{^{13}C_2H_6}R_{reference} \text{ -1})$$

and

$$\delta 31_1 = 1000 \; . \; (^{^{13}C^{12}CH_6 \; + \; ^{12}C_2DH_5 \; + \; ^{13}C_2H_5 \; + \; ^{13}C^{12}CDH_4}R_{sample}/$$
$$^{^{13}C^{12}CH_6 \; + \; ^{12}C_2DH_5 \; + \; ^{13}C_2H_5 \; + \; ^{13}C^{12}CDH_4}R_{reference} \text{ -1})$$

where ^{i}R is equal to

$$i^+/(^{12}C_2H_6^+ \; + \; ^{13}C^{12}CH_5^+ \; + \; ^{12}C_2DH_4^+)$$

Mass 30 species are collected on a 10^{11} Ω amplifier, mass 31 species on a 10^{12} Ω amplifier, and mass 32 species on an electron multiplier equipped with a retardation lens. The mass spectrometer is set to high-resolution mode and tuned to a mass resolving power of 22,000 or better. Typically, the width of the flat shoulder on mass 32 is 20 to 30 times larger than the stability of the beam position on the mass scale. This relatively wide flat shoulder is the principal motivation behind our use of wide detector apertures, which gives rise to the complexity of our background and ion correction schemes.

The exact positions on the mass scale where the signals are collected are shown on Figures S2, S3 and S4. Bellows are balanced manually in order to get a signal of ≈9 V on mass 30 for both reference and sample. This corresponds to about 2 V on mass 31, and ≈60,000 counts per seconds on mass 32. The precision of the two parts of measurement 1 are limited by counting statistics, as shown in Figure S5.

3.1.1 Background correction on mass 32

It is necessary to correct the intensity of the mass 32 signal for the methanol contribution, as described in 2.2.3. Before and after each acquisition, we measure the intensity of the methanol ion beam alone on both sample and reference side, with gas flowing in the source. This is done by changing the intensity of magnetic field to measure the intensity of the methanol ion beam (see Figure S4). We observed that this species has a long residence time in the source, and that there can be a difference of up to 300 counts per seconds between the reference and the sample side. Consequently, the manual background acquisition mimics the cycles of integration and idle time to get a representative value of the background value of methanol under the same conditions as an isotopic analysis. The intensity of the methanol ion beam is recorded for 4 minutes, switching from one bellow to the other every minute. The relevant background value is calculated by averaging the intensity recorded over the last 30 seconds of each simulated reference-sample cycle.

3.2 Measurement 2 details

For the second measurement, the detector array is configured to measure the ratio of ($^{13}C^{12}CH_6^+$ + $^{13}C_2H_5^+$ + $^{13}C^{12}CDH_4^+$) to ($^{12}C_2H_6^+$ + $^{13}C^{12}CH_5^+$ + $^{12}C_2DH_4^+$), which involves moving one Faraday cup from its position in the configuration used for Measurement 1.

The presence of fragments on both masses is corrected for during the data processing. The differences between the sample and the reference are noted, using the same δ and R notation as before, as:

$\delta 31_2 = 1000\ .\ (^{13}C^{12}CH_6 + {}^{13}C_2H_5 + {}^{13}C^{12}CDH_4 R_{\text{sample}}/$

$^{13}C^{12}CH_6$ + $^{13}C_2H_5$ + $^{13}C^{12}CDH_4 R_{reference}$ -1)

Mass 30 species are collected on a 10^{11} Ω amplifier, and mass 31 species on a 10^{12} Ω amplifier. This measurement is done in high-resolution mode. The width of the flat shoulder on mass 31 is typically 10 to 15 times larger than the stability of the beam position on the mass scale.

The position on the mass scale is unchanged for mass 30, while for mass 31 the magnetic field is adjusted to measure the leading shoulder (see Figure S3). Bellows are balanced as before (typically ≈9 V on mass 30 and ≈1.9 V on mass 31).

4 Sample handling and purification

4.1 Checking the purification procedure

To check the efficacy of our purification (focusing in particular on the efficiency of separation of CO_2 and propane from ethane), we observe the mass spectrum at mass 44, which contains peaks from both of these two gases, and compared the observed intensities for samples to those for the gas from our reference ethane tank. In medium resolution mode, the 44 amu beams for propane and CO_2 ($^{12}C_3H_8$ and $^{12}C^{16}O_2$) are fully mass resolved. For the reference gas, the signals on mass 44 from both propane and CO_2 is typically about 0.1% of the signal on mass 30 coming from ethane. For purified ethane, the propane signal is typically 0.1-0.2% of the mass 30 ethane signal while the CO_2 signal ranges from 0.1 to 1% of the mass 30 ethane signal. It should be noted that these should not be taken as direct measures of the mixing ratios of these gases in the sample, because of differences in ionization efficiency and the possibility that some species are made by fragmentation/ recombination or other source reactions.

4.2 Tests of the sample handling procedures

We performed a series of tests to verify that our sample handling does not change the isotopic composition of purified ethane (see Table S2). First, we transferred ethane among various components of the vacuum line, 5 times in a row, using liquid nitrogen traps; we find this transfer does not cause measurable changes in its isotopic composition. Likewise, an aliquot of pure ethane was subjected to our full cryogenic purification procedure, which was found to create no change in its isotopic composition, within error, from the values measured on the pure tank gas. Lastly, we created a mixture of methane, ethane and CO_2 (with approximate molar proportions 7:3:1) by freezing aliquots of each gas in the cold trap, then thawing and refreezing all gases twice. The ethane was then extracted from this mixture using the cryogenic distillation described above, and its isotopic composition was found to be within errors of the ethane used to produce the mixture. We therefore conclude that repeatedly freezing and releasing ethane with liquid nitrogen, or separating ethane from other alkanes and carbon dioxide, does not cause detectable changes in its isotopic composition.

5 Comparison of bulk isotopes with classical techniques

5.1 Carbon

Samples were injected into a gas chromatograph using helium as a carrier gas, converted to CO_2 by combustion and then analysed on a mass spectrometer in continuous-flow mode. We report in Table S3 and Figure S6 the $\delta^{13}C$ measured with both techniques. All the values are relative to the PDB scale.

To take into account the different errors from the conventional techniques and the technique developed here, we performed a York-type regression, where errors in both axes are taken into account. The slope of the line is equal to 1.005 ± 0.009 ($1\ \sigma$) and the intercept of the line is 0.24 ± 0.28 ($1\ \sigma$). Thus the fit line is statistically indistinguishable from a 1:1 line.

5.2 Hydrogen

After injection of the analyte into a gas chromatograph, ethane was pyrolysed to produce H_2, which was analysed on a mass spectrometer in continuous flow mode. At Caltech, the analysis of the samples' δD was done after separating ethane from other species as described earlier, while at Isotech the different species are separated by gas chromatography. The comparison between the GC-IRMS and the Ultra data is reported in Table S4 and Figure S7. All the values are reported on the SMOW scale. The slope of the line is equal to 1.06 $\pm$ 0.05 ($1\ \sigma$) and the intercept of the line is 9.0 ± 6.7 ($1\ \sigma$). Within $2\ \sigma$, the fit line is indistinguishable from a 1:1 line, suggesting no systematic artefacts. There is more scatter than expected based on the nominal precision of each method. It is difficult to evaluate the cause of this scatter, though we note that the conventional measurement of δD of ethane has not been subjected to a rigorous study of interlaboratory standardisation (in fact, we are not aware of any widely distributed interlaboratory standards). Therefore, it seems possible to us that some unrecognised irreprodicibility in the GC separation and/or online reduction of ethane may account for a part of the scatter in Figure S7.

6 Calculation of δD, δ^{13}C and $\Delta^{13}C_2H_6$

Due to the presence of non-negligible amounts of fragments at mass 30 and mass 31, the calculation of the isotopic composition cannot be done directly. An iteration method is necessary.

We have described above how the fragmentation ratio, F, is calculated (see the subsection 2.4). The isotopic ratios measured on mass 31 can then be written as follows :

$$^{13}C^{12}CH_6 + {}^{12}C_2DH_5 + {}^{13}C_2H_5 + {}^{13}C^{12}CDH_4R =$$

$$([^{13}C^{12}CH_6] + [^{12}C_2DH_5] + F([^{13}C_2H_6] + 5/6[^{13}C^{12}CDH_5])) /$$

$$([^{12}C_2H_6] + F([^{13}C^{12}CH_6] + 5/6[^{12}C_2DH_5]))$$

and

$$^{13}C^{12}CH_6 + {}^{13}C_2H_5 + {}^{13}C^{12}CDH_4R =$$

$$([^{13}C^{12}CH_6] + F([^{13}C_2H_6] + 5/6[^{13}C^{12}CDH_5])) /$$

$$([^{12}C_2H_6] + F([^{13}C^{12}CH_6] + 5/6[^{12}C_2DH_5]))$$

F is typically equal to 0.81, with a range of $\pm$ 0.025 observed over 18 months of measurements. We have assumed that the fragmentation ratio is identical for all isotopologues of ethane. Assuming that the isotopes are randomly distributed, we can rewrite these equations as :

$$^{13}C^{12}CH_6 + {}^{12}C_2DH_5 + {}^{13}C_2H_5 + {}^{13}C^{12}CDH_4R =$$

$$(2[^{13}C][^{12}C][H]^6 + 6[^{12}C]^2[D][H]^5 + F([^{13}C]^2[H]^6 + 10[^{13}C][^{12}C][D][H]^5))/$$

$$([^{12}C]^2[H]^6 + F(2[^{13}C][^{12}C][H]^6 + 5[^{12}C]^2[D][H]^5]))$$

and

$$^{13}C^{12}CH_6 + {}^{13}C_2H_5 + {}^{13}C^{12}CDH_4R =$$

$$(2[^{13}C][^{12}C][H]^6 + F([^{13}C]^2[H]^6 + 10[^{13}C][^{12}C][D][H]^5))/$$

$$([^{12}C]^2[H]^6 + F(2[^{13}C][^{12}C][H]^6 + 5[^{12}C]^2[D][H]^5]))$$

These equations can be simplified to :

$^{13}C^{12}CH_6$ + $^{12}C_2DH_5$ + $^{13}C_2H_5$ + $^{13}C^{12}CDH_4$R =

$(2^{13}R + 6^{D}R + F(^{13}R^2 + 10^{D}R^{13}R))/(1+F(2^{13}R + 5^{D}R))$

and

$^{13}C^{12}CH_6$ + $^{13}C_2H_5$ + $^{13}C^{12}CDH_4$R =

$(2^{13}R + F(^{13}R^2 + 10^{D}R^{13}R))/(1+F(2^{13}R + 5^{D}R))$

Likewise, for the 32/30 ratio, we have

$^{13C_2H_6}R = [^{13}C_2H_6] / ([^{12}C_2H_6] + F([^{13}C^{12}CH_6] + 5/6[^{12}C_2DH_5]))$

The only exception here is that the isotopes in $[^{13}C_2H_6]$ are not assumed to be randomly distributed. With the definition of $\Delta^{13}C_2H_6$ we gave, this equation can be rewritten as :

$^{13C_2H_6}R = (([^{13}R)^2.(1+\Delta^{13}C_2H_6/1000)) / (1+F(2^{13}R + 5^{D}R))$

Those three equations are then solved iteratively with a Matlab script to find the ^{D}R, ^{13}R and $\Delta^{13}C_2H_6$ of the sample. It should be noted that it is assumed that the isotopes are distributed randomly among all isotopologues in the reference gas, although if they were not the offsets in the $\Delta^{13}C_2H_6$ calculated for natural samples would be negligible. The exact value of $^{13C_2H_6}R$ for the reference is not known, and as explained in this paper is difficult to tie an external reference frame because of the chemical properties of ethane.

To calculate the precision of the ^{D}R, ^{13}R and $\Delta^{13}C_2H_6$ of the sample, we use a Monte-Carlo method where we create artificial distributions of the δ values measured from their averages and internal precisions.

7 Mixing Experiment

We present the results of a mixing experiment conducted early in the course of this study where we added small amounts of ethane labelled as 99% $^{13}CH_3$-

$^{12}CH_3$ to our reference gas (Figure S8). The labelled gas was added to aliquots of the reference gas using the vacuum line, by freezing both in liquid nitrogen. Due to the nature of the valves used on the vacuum line and bulb containing the labelled gas (Teflon screw valves), the ratios of the two gases were not precisely measured. We observe that the $\Delta^{13}C_2H_6$ value of the gas decreases with further addition of the labelled gas (seen through the $\delta^{13}C$ of the mixture). We model the expected evolution in $\delta^{13}C$-$\Delta^{13}CH_6$ space depending on the real composition of the labelled gas, assuming that the amount of $^{12}CH_3$-$^{12}CH_3$ in the added labelled gas was negligible and that the distribution of isotopes was stochastic in our reference gas. Depending on the proportion of $^{13}C_2H_6$ present in the labelled gas, mixing curves in $\delta^{13}C$-$\Delta^{13}CH_6$ space differ strikingly. The isotopic compositions measured are consistent with 1.1% of the labelled gas being $^{13}C_2H_6$. Note that the error bars (shown at the 2 σ level) in the graph are much larger than those for the other measurements shown in this paper as this was a preliminary, proof of concept experiment.

Bibliography

References

[Friedman, 1953] Friedman, I. (1953). Deuterium content of natural waters and other substances. *Geochimica et Cosmochimica Acta*, 4(1):89–103.

[Stolper et al., 014a] Stolper, D., Sessions, A., Ferreira, A., Neto, E. S., Schimmelmann, A., Shusta, S., Valentine, D., and Eiler, J. (2014a). Combined ^{13}C–D and D–D clumping in methane: Methods and preliminary results. *Geochimica et Cosmochimica Acta*, 126:169–191.

8 Tables

8.1 Table S1

Isotopic compositions of a gas measured at a range of pressures.

Intensity on mass 30 (V)	δ^{13}C (‰)	err (‰)	δD (‰)	err (‰)
6.4	-10.91	0.02	-116.13	0.56
9.3	-10.95	0.02	-115.88	0.56
10	-10.95	0.02	-115.63	0.52
12	-10.90	0.05	-116.00	1.22

8.2 Table S2

Sample handling experiments. We compare isotopic compositions obtained during a typical 0-enrichment, where our reference gas is compared to itself, to those obtained after two different handling procedures. See text for details.

	δ^{13}C (‰)	err (‰)	δD (‰)	err (‰)	$\Delta^{13}C_2H_6$ (‰)	err (‰)
Typical 0-enrichment	-24.50	0.02	-108.98	0.49	0	0.1
5 recaptures	-24.48	0.03	-108.75	0.59	0.13	0.16
Separation process	-24.48	0.02	-108.97	0.54	-0.09	0.12
Mixture separation	-24.51	0.03	-109.21	0.48	-0.06	0.10

8.3 Table S3

Comparison of independent δ^{13}C measurements from established techniques and measurements on the Ultra. [a] : samples measured by Isotech, [b] : samples measured at PEERI (see text for details).

$\delta^{13}C_{external}$ (‰)	err (‰)	$\delta^{13}C_{Ultra}$ (‰)	err (‰)
-40.6[a]	0.3	-40.29	0.06
-42.03[a]	0.3	-42.32	0.08
-38.14[a]	0.3	-38.20	0.06
-34.25[a]	0.3	-34.23	0.02
-19.88[a]	0.3	-19.27	0.07
-21.28[a]	0.3	-20.78	0.07
-10.1[b]	0.25	-10.21	0.03
-25.09[b]	0.25	-25.20	0.06

8.4 Table S4

Comparison of independent δD measurements from established techniques and measurements on the Ultra. [a] : samples measured by Isotech, [b] : samples measured at Caltech (see text for details).

$\delta D_{external}$ (‰)	err (‰)	δD_{Ultra} (‰)	err (‰)
-183.5[a]	5	-177.5	0.6
-189.1[a]	5	-196.1	0.5
-179.4[a]	5	-181.8	0.6
-109.7[a]	5	-96.4	0.7
-109.6[a]	5	-100.1	0.7
-171.1[a]	5	-167.0	1.0
-127.0[b]	1.5	-128.1	0.4
-120.7[b]	1.5	-121.7	1.4

9 Figure captions

9.1 Figure S1

Ionization spectrum of ethane by the source of the mass spectrometer, with tuning conditions maximising the intensity on mass 30. The mass with the highest signal is mass 28, mainly due to $C_2H_4^+$, illustrating the loss of hydrogen atoms from the ethane molecule. Peaks at m/z = 14.5 and 13.5 show that doubly-charged ions are created (respectively mostly $C_2H_5^{2+}$ and $C_2H_3^{2+}$).

9.2 Figure S2

Mass spectrum at mass 30, measured at high resolution (22,000-23,000 mass resolving power) on a Faraday cup linked to a 10^{11} Ω resistor.

9.3 Figure S3

Mass spectrum at mass 31, measured at high resolution (22,000-23,000 mass resolving power) on a Faraday cup linked to a 10^{12} Ω resistor. The partial mass spectrum was measured using a 0.5 s integration time at each magnet position and a 0.5 s idle time to prevent the rounding of the features due to the use of a 10^{12} Ω resistor. It demonstrates that $^{13}C^{12}CH_6$ can be resolved from $^{12}C_2DH_5$. Measurements 1 and 2 refer to the two measurements described in Section Description of the analytical procedures.

9.4 Figure S4

Mass spectrum at mass 32, measured at high resolution (22,000-23,000 mass resolving power) on a secondary electron multiplier equipped with a retarda-

tion lens. O_2 is cleanly resolved from the ethane isotopologues. The partial mass spectrum documenting the low-mass shoulder shows that $^{13}C_2H_6$ can be resolved from $^{13}C^{12}CDH_5$.

9.5 Figure S5

Comparison of the internal precision of a typical measurement to the theoretical limits due to counting statistics. Measurements are shown after background corrections (circles). Theoretical limits are shown as solid lines. a) Measurement of $\delta^{13}C_2H_6$. The precision approach 0.11‰ after 80 cycles. b) Measurement of $\delta 31_1$ where mass 31 includes both $^{13}C^{12}CH_6$ and $^{12}C_2DH_5$. After 80 cycles, the precision is close to 0.007‰. c) Measurement of $\delta 32_2$ where mass 31 includes $^{13}C^{12}CH_6$. After 24 cycles, the precision approaches 0.019‰.

9.6 Figure S6

Comparison of $\delta^{13}C$ measurements made on the Ultra or using conventional techniques (conversion to CO_2). See text for details on the type of regression used. Error bars are smaller than the symbols on both axis.

9.7 Figure S7

Comparison of δD measurements made on the Ultra or using conventional techniques (conversion to H_2). See text for details on the type of regression used. Error bars on the y axis are smaller than the symbols.

9.8 Figure S8

Mixing experiment: addition of small amounts of 99% $^{13}CH_3$-$^{12}CH_3$ gas to our reference gas. The axis are vs the reference gas composition rather than vs PDB in this figure. Lines described the expected variations in clumped signature depending on the percentage of $^{13}CH_3$-$^{13}CH_3$ contained in the labelled gas. The error bars are equal to 2σ.

10 Figures

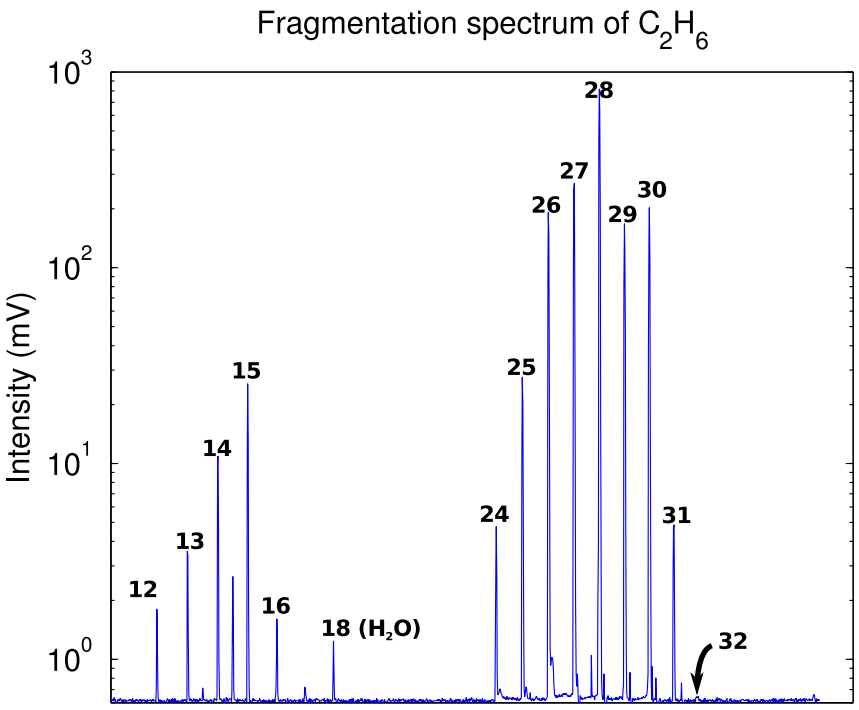

Figure 1: Figure S1.

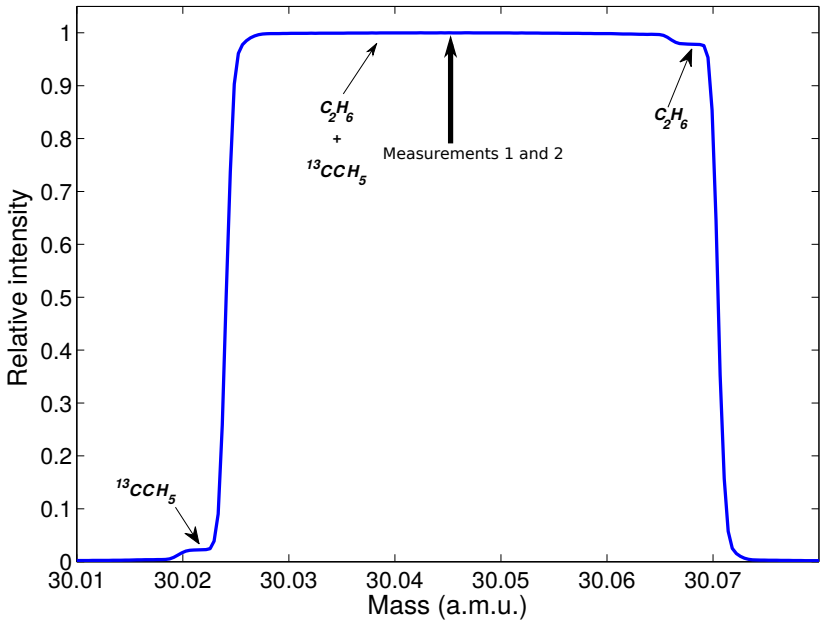

Figure 2: Figure S2.

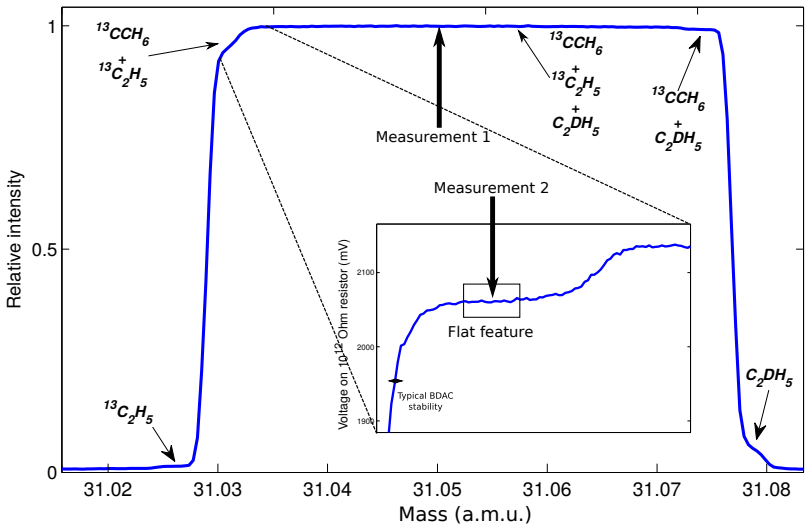

Figure 3: Figure S3.

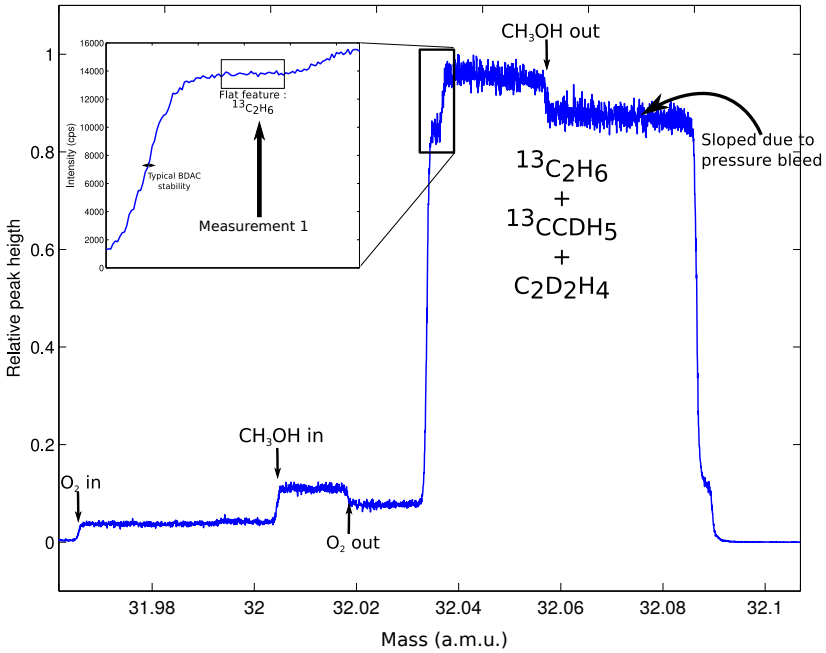

Figure 4: Figure S4.

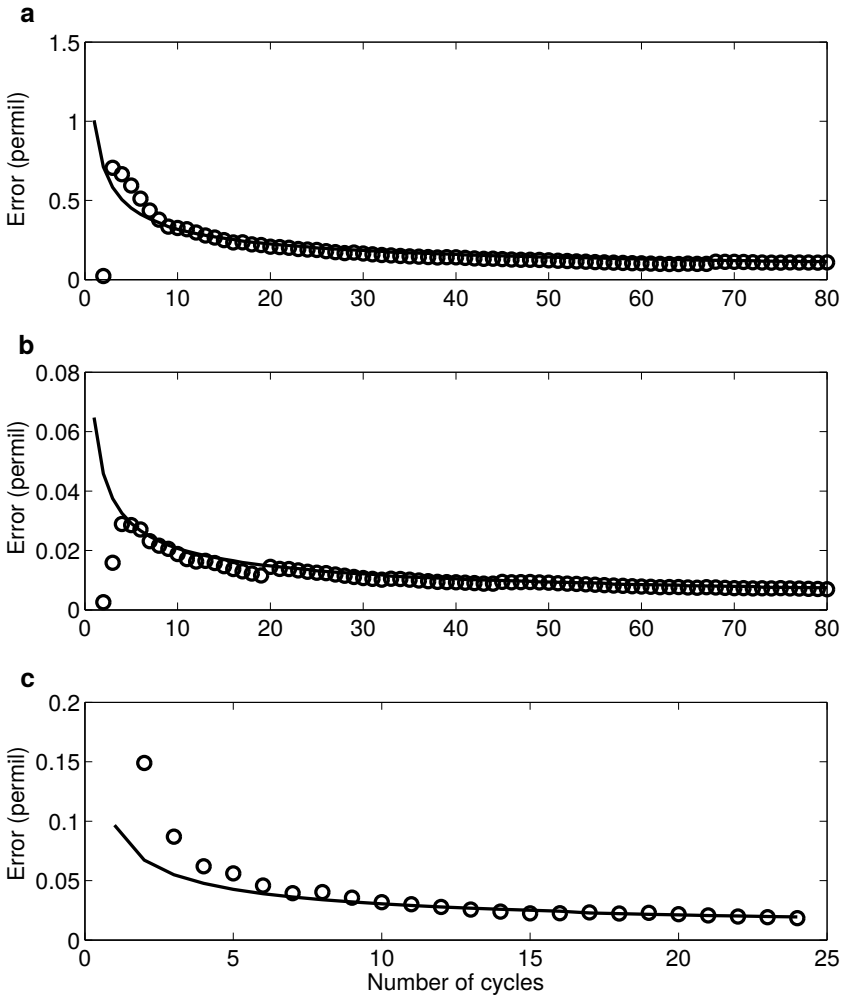

Figure 5: Figure S5.

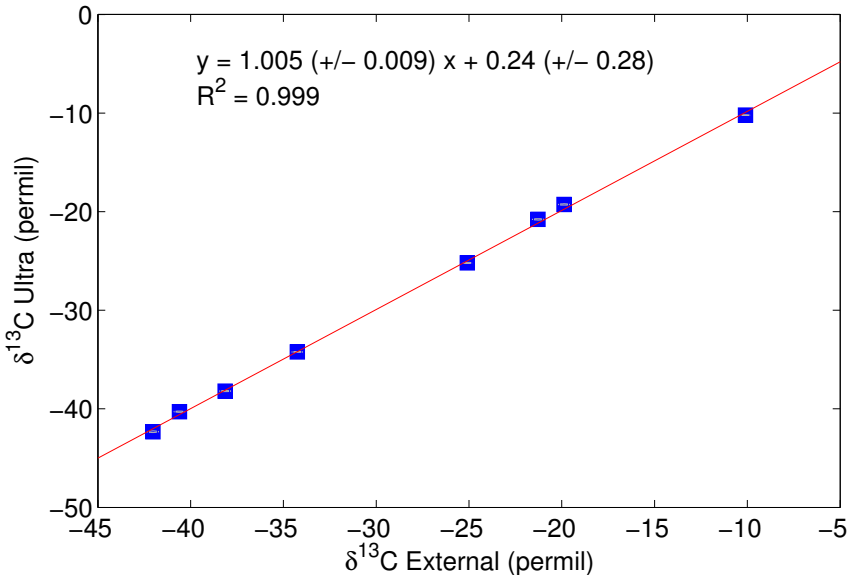

Figure 6: Figure S6.

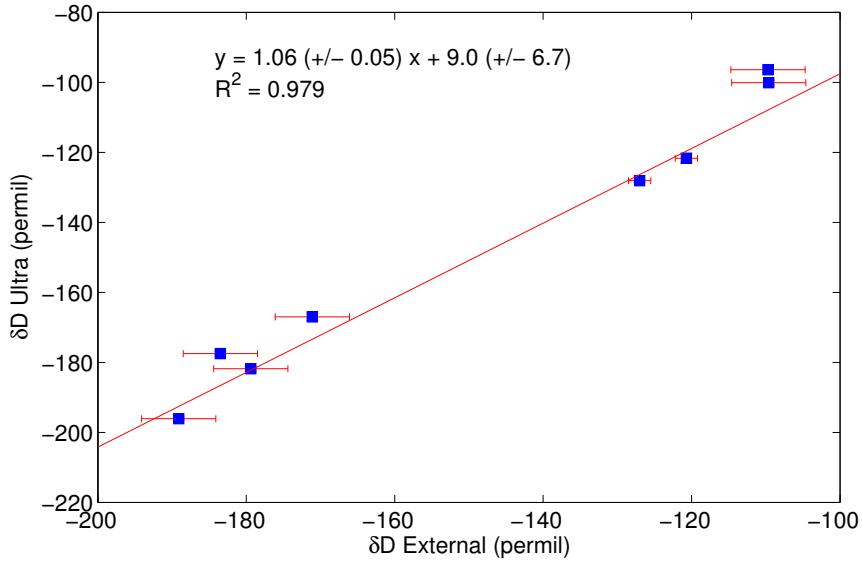

Figure 7: Figure S7.

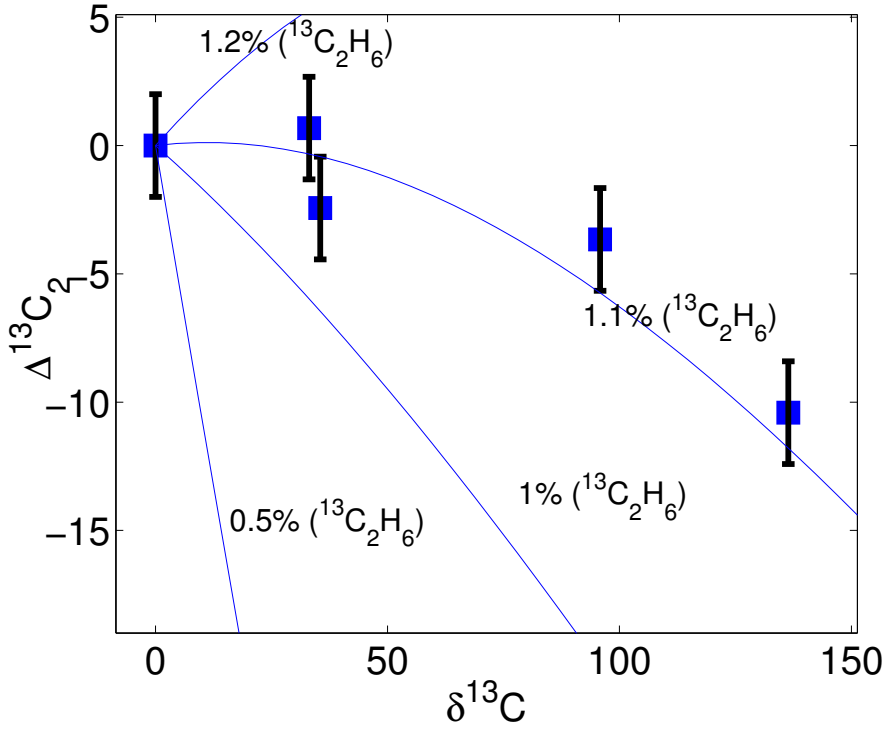

Figure 8: Figure S8.